Journal of Power Sources 248 (2014) 1085–1089

Contents lists available at ScienceDirect

Journal of Power Sources

journal homepage: www.elsevier.com/locate/jpowsour

Short communication

Molecular dynamics simulation of the effect of dopant distribution homogeneity on the oxide ion conductivity of Ba-doped $LaInO_3$

Mi-Young Yoon [a], Kuk-Jin Hwang [a,b], Dae-Seop Byeon [c], Hae-Jin Hwang [a,**], Seong-Min Jeong [b,*]

[a] School of Materials Science and Engineering, Inha University, 253 Yonghyun-dong, Nam-gu, Incheon 402-751, Republic of Korea
[b] Korea Institute of Ceramic Engineering and Technology, 233-5 Gasan-dong, Guemcheon-gu, Seoul 153-801, Republic of Korea
[c] Department of Materials Science and Engineering, Yonsei University, 50 Yonsei-ro, Seodaemun-gu, Seoul 120-749, Republic of Korea

HIGHLIGHTS

- Oxide ion conduction of $La_{0.6}Ba_{0.4}InO_{2.8}$ was analyzed by a MD simulation.
- The calculations showed that ion conduction depends on the Ba dopant distribution.
- Ionic conductivity increased with increasing homogeneity of the Ba dopant in $LaInO_3$.
- Deviations of the ionic conductivities were strongly affected by the dopant distribution.

ARTICLE INFO

Article history:
Received 17 August 2013
Received in revised form
26 September 2013
Accepted 14 October 2013
Available online 21 October 2013

Keywords:
Molecular dynamics
Oxide ion conductor
Solid oxide fuel cell
Perovskite oxide
Dopant distribution

ABSTRACT

Molecular dynamics simulations are conducted to study oxide ion conduction in Ba-doped $LaInO_3$, a type of cubic perovskite oxide. In a previous study, we reported that the Ba dopant forms oxygen vacancies and narrow bottlenecks that function as a barrier to the movement of oxide ions. In this further study, we analyze the effects of dopant distribution on the oxide ion conductivity in Ba-doped $LaInO_3$. The results show that the ionic conductivity of Ba-doped $LaInO_3$ is strongly dependent on the dopant distribution. The Ba-rich region plays a crucial role in decreasing the ionic conductivity. Consequently, a homogeneous dopant distribution without a Ba-rich region is estimated to improve the ionic conductivity of Ba-doped $LaInO_3$.

1. Introduction

Yttria-stabilized zirconia (YSZ) shows good performance as an electrolyte material in solid oxide fuel cells (SOFCs) at high temperatures (>800 °C). At intermediate temperatures (600–800 °C), however, an optimal material for use as a SOFCs electrolyte has still not been developed. ABO_3 perovskite, with substitutional cation dopants, has the potential to exhibit oxide or proton conduction because the substituted cations produce oxygen vacancies or protons as the charge carriers. For applications as an electrolyte in SOFCs, ABO_3 perovskite should be doped with substitutional cations to acquire oxide conduction characteristics. In particular, many researchers have studied La-based ABO_3 perovskite as a promising oxide conductor applicable as the electrolyte in SOFCs at intermediate temperatures owing to its high ionic conductivity, phase stability and process feasibility at intermediate temperatures [1–5].

The oxide ion conduction of ABO_3 perovskite is governed by many factors including the species and amount of dopant cations characterized by the tolerance factor [2,4,6]. Although the tolerance factor could provide a simplified way of characterizing a "superficial" lattice structure, it cannot provide insights into the determination of the ionic movement in the lattice structure, which is affected by a variety of factors including the species and amount of dopant cations. Furthermore, the increase in oxygen vacancies by cation doping does not always improve the oxide conduction of ABO_3 perovskite, as Kakinuma et al. reported for the behavior of (La,

* Corresponding author. Tel.: +82 2 3282 7825; fax: +82 2 3282 2490.
** Corresponding author. Tel.: +82 32 860 7521; fax: +82 32 862 4482.
E-mail addresses: hjhwang@inha.ac.kr (H.-J. Hwang), smjeong@kicet.re.kr (S.-M. Jeong).

0378-7753/$ – see front matter © 2013 Elsevier B.V. All rights reserved.
http://dx.doi.org/10.1016/j.jpowsour.2013.10.054

Ba)InO_3 perovskite [7]. They explained this phenomenon by introducing the concept of a "mobile oxide ion", which means that only a fraction of the oxide ions can act as the conducting carriers due to the association effect [7]. Dopant distribution has also been suspected as being a major source of the large deviations in the ionic conductivity of SOFC electrolyte. Yamamura et al. [8] and Tarancón et al. [9] analyzed the effects of dopant distribution on the diffusion behavior of oxide ions in YSZ with a fluorite structure by molecular dynamics (MD) simulations. Both groups confirmed that the particular configuration of the dopant improved the electrical properties of YSZ. On the other hand, the effect of dopant distribution on oxide ion conductivity in perovskite oxide has not been evaluated.

In our previous study, the conduction pathways of oxide ions in Ba-doped $LaInO_3$ perovskite were monitored carefully and analyzed by MD simulations [10]. $La_{1-x}Ba_xInO_{3-0.5x}$ oxides have different crystal symmetries of perovskite, depending on the Ba content. It was found to exist as cubic and orthorhombic phases in the case where $x = 0.1$–0.3, and as a cubic single phase where $x = 0.4$–0.5 and a tetragonal phase where $x = 0.6$ [7,17]. Kim et al. investigated the electrical conduction behavior of Ba-doped $LaInO_3$ and reported that the oxide has pure oxide ion conduction characteristics under a dry N_2 atmosphere [17]. The concept of a "bottleneck" was introduced to describe the barrier against the migration of oxide ions from a structural point of view. The critical radius of the bottleneck as a pathway was found to be a major determinant in the migration of oxide ions between adjacent octahedral sites. This suggests that the ionic conductivity is dependent on the distribution of dopant cations. Therefore, in the present study, MD simulations were performed to analyze the effect of the dopant distribution on the oxide ion conductivity of Ba-doped $LaInO_3$ perovskite.

2. Method of calculation

The interatomic potentials used in this study were the Born model framework consisting of a Coulombic term, a short range repulsion term and a dispersion term as follows:

$$U_{ij} = \frac{q_i q_j}{r_{ij}} + f_0(b_i + b_j)\exp\left[\frac{a_i + a_j - r_{ij}}{b_i + b_j}\right] - \frac{c_i c_j}{r_{ij}^6} \quad (1)$$

where q_i and q_j are the charges of two ions i and j, respectively, separated by the distance r_{ij}. f_0 is a constant for unit adaptation ($=1$ kcal mol^{-1} Å^{-1}). a, b and c are parameters for each ion, in which values were listed in the previous studies [11,12]. All calculations were carried out using the parallel-processing MD simulation package, LAMMPS (Sandia National Laboratory, USA) [13,14].

The simulation model consisted of 200 unit cells with a total of 960 atoms corresponding to the composition, $La_{0.6}Ba_{0.4}InO_{2.8}$. The oxygen vacancies were generated manually by removing an oxide ion in the selected octahedral sites to maintain charge neutrality. In our previous study, a bottleneck is defined as a triangle with two *A*-site cations and one *B*-site cation, as shown in Fig. 1. For Ba-doped $LaInO_3$, there are two types of *A*-site cations, La, and Ba, and only one *B*-site cation species, In. Only three types of bottlenecks exist; ΔLaLaIn, ΔLaBaIn and ΔBaBaIn. The bottlenecks were characterized by their critical radii, r_{crit}, as calculated using values of 1.072 Å, 0.964 Å and 0.868 Å for ΔLaLaIn, ΔLaBaIn and ΔBaBaIn, respectively. Four models with different Ba dopant distributions were used to analyze the effect of the dopant distribution on the oxide ion conductivity. Table 1 shows the four models characterized with their constituting bottlenecks. As reported in our previous study, the bottleneck types depend on the arrangement of atoms at the A-site positions [10]. Therefore, the four models with different

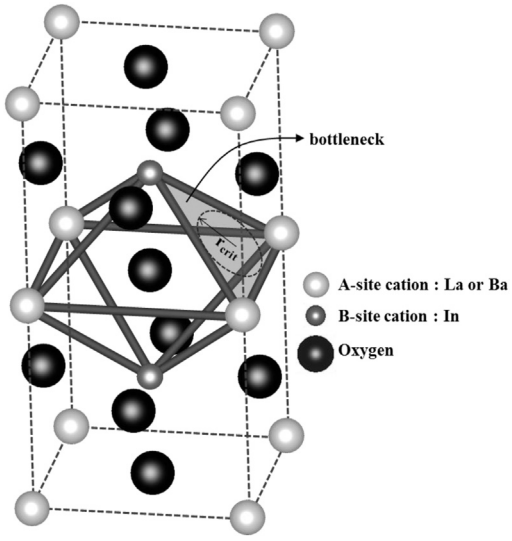

Fig. 1. ABO_3 perovskite structure showing octahedral sites for oxide ions.

amounts of bottleneck values were obtained by the manual arrangement of La and Ba.

Before the main simulations, relaxation steps were carried out at 298 K under a constant pressure of 1 atm for 0.4 ns with a time step of 1 fs using the NPT ensemble. The main simulation was performed at 1173–1473 K for 1.6 ns to obtain the mean square displacement (MSD) curves for each element. Finally, the ionic conductivities and activation energies were derived from the diffusion coefficient of oxide ion according to the Nernst–Einstein relationship [15,16]. Details of each of the calculations performed in the present study were identical to those from our previous study [10]. As described in the previous study, the lattice parameter of $La_{0.6}Ba_{0.4}InO_{2.8}$ using the Born framework showed good agreement with the experimental values [17].

3. Results and discussion

According to our calculations for 1073 K, the probabilities of oxygen migrations through the bottlenecks were calculated to be 90%, 10% and 0% for ΔLaLaIn, ΔLaBaIn and ΔBaBaIn, respectively [10]. This shows that oxide ion diffusion occurs mainly through ΔLaLaIn and ΔLaBaIn, and not through ΔBaBaIn, which has the smallest critical radius. Therefore, the effective pathways in Ba-doped $LaInO_3$ are assumed to be both ΔLaLaIn and ΔLaBaIn. When more Ba ions are doped in $LaInO_3$, more ΔBaBaIn is formed with more oxygen vacancies and less ΔLaLaIn. This can explain why the increase in Ba in $LaInO_3$ causes a decrease in ionic conductivity despite the increase in oxygen vacancies, as described in detail in our previous study [10]. In other words, a decrease in the effective pathways was found to compensate for the increase in oxygen vacancies and decrease in ionic conductivity.

ΔBaBaIn must be formed in a "Ba-rich" region, particularly in the lattice structure with an inhomogeneous distribution of the Ba

Table 1
Configurations of the different dopant homogeneity characterized by the amount of bottleneck type.

Bottleneck type	Configuration			
	A	B	C	D
ΔLaLaIn	808	812	828	836
ΔLaBaIn	1264	1256	1224	1208
ΔBaBaIn	328	332	348	356

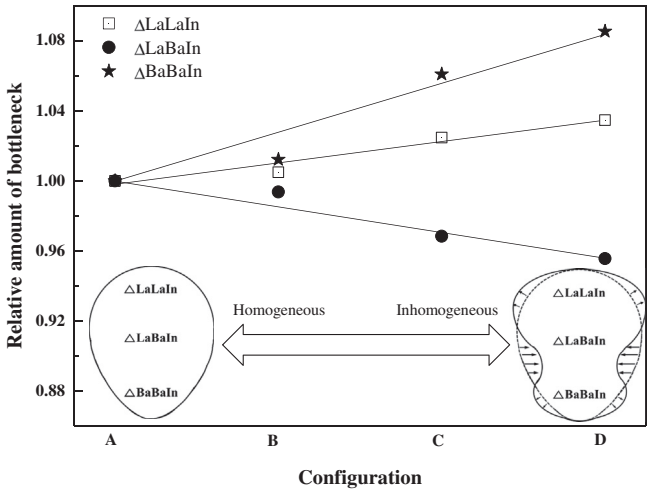

Fig. 2. Change in the dopant homogeneity characterized by the relative amount of bottleneck types.

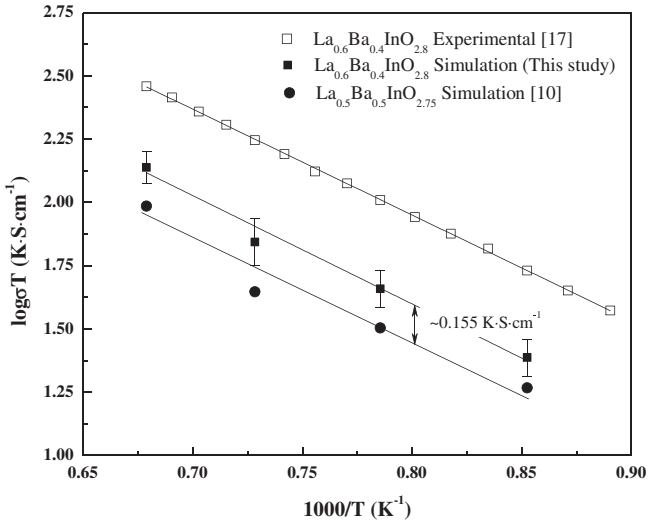

Fig. 3. Arrhenius plots of the calculated oxide ion conductivities of Ba-doped $LaInO_3$ with previous experimental results.

dopant. Therefore, four different configurations were prepared in order to analyze the effects of dopant distribution on ionic conductivity. The difference in each configuration was quantified with their amounts of bottlenecks, as shown in Table 1. While more Ba dopant in $LaInO_3$ forms more ΔBaBaIn and less ΔLaLaIn, more ΔBaBaIn means more ΔLaLaIn under a composition with a constant amount of Ba dopant because the formation of a "Ba-rich" region inevitably results in the simultaneous formation of a "La-rich" region. Consequently, the variation of ΔBaBaIn according to the configurations are equal to that of ΔLaLaIn. Because the current study is for a La-rich composition, $La_{0.6}Ba_{0.4}InO_{2.8}$, the absolute amount of ΔLaLaIn must be more than that of ΔBaBaIn. The varied amount of each bottleneck could be normalized by dividing its absolute amount to quantify the effect of the dopant distribution. Therefore, the amounts of each bottleneck types in each configuration were divided by the amounts of the corresponding bottleneck types in configuration A to produce the relative values. Fig. 2 shows that the relative amounts of ΔBaBaIn are higher than that of ΔLaLaIn, and an increase in the amount of ΔLaLaIn and ΔBaBaIn mean a decrease in the amount of ΔLaBaIn. Configurations with more ΔLaLaIn and ΔBaBaIn became closer to a dumbbell-like shape than configurations with more ΔLaBaIn, as shown in Fig. 2.

Fig. 3 shows the ionic conductivities calculated in the present study at temperatures of 1173–1473 K. The experimental ionic conductivity is generally lower than the calculated value because ionic conductivity is affected by grain boundaries, impurities, pores and other experimental issues. However, as shown in Fig. 3, the calculated ionic conductivity was lower than the experimental value, which was estimated by the imperfections in the interatomic potential, as reported in previous study employing Born-Mayer potential [22,23]. Of course, if the goal of the study was to obtain values for the ideal ionic conductivity, it would be necessary to prepare interatomic potentials capable of obtaining precise values. However, the goal of this study was not the acquisition of the precise ideal ionic conductivity, but to develop further insights into the ionic conduction behavior in perovskite oxide. The simulations employing Born Mayer potential provided small deviation in the ionic conductivities and activation energies in the Ba-doped $LaInO_3$ [10]. Therefore, the calculations with the Born Mayer potential were assumed to be sufficiently reliable to meet the goal of the study. Interestingly the calculated ionic conductivities showed remarkable standard deviations ranging from 0.062 to 0.094 K S cm^{-1} under all temperature conditions. The experiments were subject to some uncertainty because a wide range of errors and inaccuracies always occur. Therefore, the experimental data would be expected to have a significant deviation from the limited accuracy of the measuring apparatus, limitations and simplifications of the experimental procedure, and uncontrolled changes to the environment. On the other hand, the simulation can exclude the listed sources of data uncertainty and permit the pure effect of the processing conditions to be evaluated. Therefore, the deviations shown in Fig. 3 indicate the magnitude of the effect of the dopant distribution with the standard deviation. According to our previous study, the calculated ionic conductivities at 1273 K of $La_{0.6}Ba_{0.4}InO_{2.8}$ and $La_{0.5}Ba_{0.5}InO_{2.75}$ were 1.658 K S cm^{-1} and 1.503 K S cm^{-1}, respectively. Experimental results reported in the previous study are consistent with $La_{0.6}Ba_{0.4}InO_{3-\delta}$ having a higher electrical conductivity than $La_{0.5}Ba_{0.5}InO_{3-\delta}$ [7]. The standard deviations obtained by varying the dopant distribution were in excess of ~40% of the difference between the ionic conductivities of $La_{0.6}Ba_{0.4}InO_{2.8}$ and $La_{0.5}Ba_{0.5}InO_{2.75}$, which showed evidence of the strong effect of the dopant distribution on the ionic conductivity of Ba-doped $LaInO_3$.

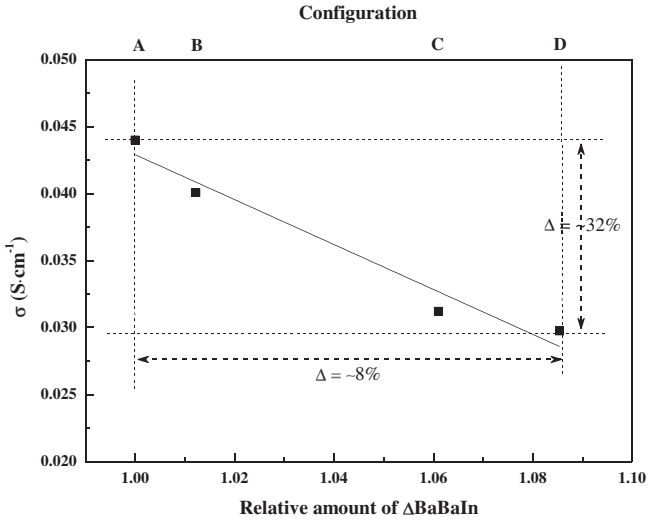

Fig. 4. Ionic conductivities of $La_{0.6}Ba_{0.4}InO_{2.8}$ at 1273 K by the relative amount of ΔBaBaIn bottlenecks. (The straight line is intended to act as a visual guide.)

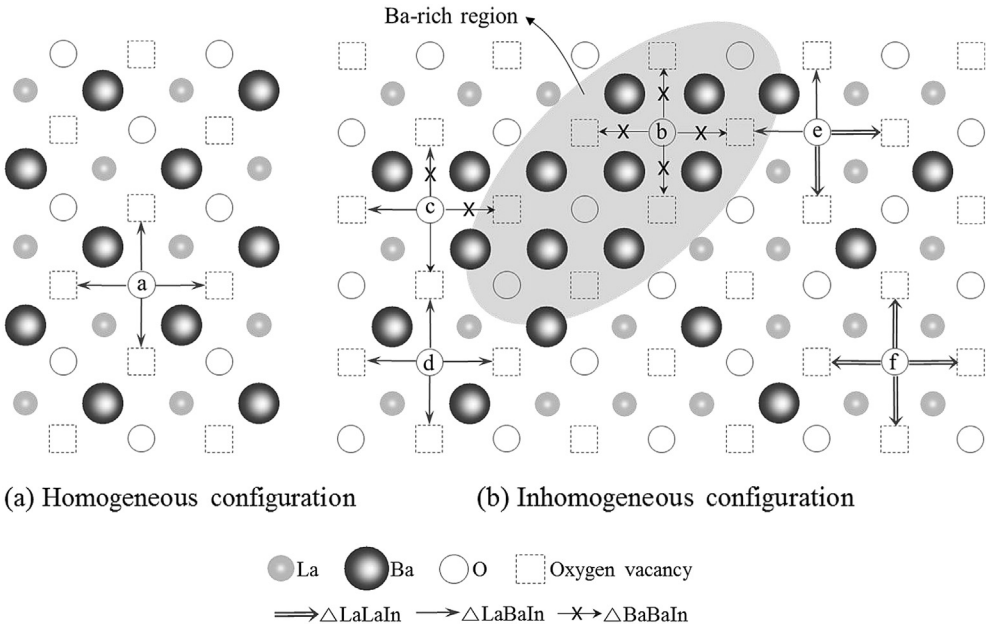

Fig. 5. Schematic diagram of oxide ion diffusion through the bottlenecks with the distribution of dopant.

Fig. 4 shows the ionic conductivity of $La_{0.6}Ba_{0.4}InO_{2.8}$ oxide at 1273 K as a function of the relative amount of ΔBaBaIn, as shown in Fig. 2. When the amount of ΔBaBaIn was found to increase by as much as 8%, the ionic conductivity to decrease by as much as 32%. This result is quite interesting because more ΔBaBaIn indicates more ΔLaLaIn at the same time. Therefore, the oxide ion conductivity of Ba-doped $LaInO_3$ is determined not by the amount of ΔLaLaIn, but by that of ΔBaBaIn. As ΔBaBaIn will exist more in the "Ba-rich" region, it is concluded that a homogeneously distributed Ba dopant is favored to achieve high ionic conductivity in Ba-doped $LaInO_3$. Therefore, the homogeneity of the dopant distribution is one of the major sources of oxide ion conductivity in perovskite.

Based on the calculation results, Fig. 5 shows a schematic diagram of oxide ion conduction in the lattice structure. In the homogeneous configuration without the Ba-rich region shown in Fig. 5(a), there are only ΔLaBaIn and oxide ion "a" could move to any adjacent site without barriers. In an inhomogeneous configuration, however, there is a Ba-rich region where the concentration of Ba ions is relatively high and an oxide ion is surrounded by only Ba cations, as shown in position "b". In this case, the oxide ion could not pass through the ΔBaBaIn to migrate to the adjacent sites, which means that the oxide ion at position "b" is immobile. On the other hand, the oxide ions at positions "c", "d", "e", and "f" are mobile because they have at least one pathway to migrate to the adjacent sites. This suggests that the inhomogeneous distribution of Ba results in the formation of a localized Ba-rich region that blocks the migration of ions to the adjacent sites. According to the calculations, the Ba-rich region acts as a so called "dead cell" that does not allow ionic diffusion. Therefore, an increase in the Ba-rich region degrades the ionic conductivity by reducing the effective diffusion pathway of oxide ions.

Furthermore, the calculation results suggest that the homogeneous distribution of Ba dopant in $LaInO_3$ oxide is favored to obtain higher oxide ion conductivity. Experimentally, a pure oxide ionic conductor, $La_{1-x}Sr_xGa_{1-y}Mg_yO_{3-0.5(x+y)}$ oxide, showed a higher conductivity when it was synthesized using a regenerative sol–gel method rather than when a conventional solid state reaction was used [18]. It appears that the merit of the sol–gel method is that it permits an inhomogeneous system to be transformed into a homogeneous system. The higher electrical conductivity of perovskite produced using the sol–gel method was explained by the better homogeneity of the dopant distribution because the sol–gel method produces relatively a high purity and homogeneous mixture on the atomic scale with fine particles, whereas the conventional solid state reaction produces an inhomogeneous dopant distribution with coarse particles due to the high calcination temperature and diffusion velocity gradient among ions [18–21]. The experimental findings [18–21] provide a clue as to which process is favored to obtain better performance in a pure oxide ionic conductor. The present study is meaningful because it provides a theoretical explanation of how the electrical conductivity of perovskite oxide is improved with a homogeneous dopant distribution.

4. Conclusions

Theoretical analysis employing a MD simulation revealed the effect of the dopant distribution on the oxide ion conductivity in Ba-doped $LaInO_3$ with a perovskite structure. The calculated ionic conductivities increased with the improved homogeneity of the Ba dopant in $LaInO_3$ due to the decrease in ΔBaBaIn. The homogeneity of the dopant distribution, which was quantified by the amount of ΔBaBaIn was found to be the governing factor determining the oxide ion conductivity of Ba-doped $LaInO_3$.

Acknowledgments

This work was supported by the National Research Foundation of Korea (NRF) grant funded by the Korean Government (MEST) (No. 2011-0015512).

References

[1] S. Wang, Y. Jiang, Y. Zhang, J. Yan, W. Li, Solid State Ionics 113–115 (1998) 291–303.
[2] D. Lybye, F.W. Poulsen, M. Mogensen, Solid State Ionics 128 (2000) 91–103.
[3] P. Huang, A. Petric, J. Electrochem. Soc. 143 (1996) 1644–1648.
[4] K. Nomura, S. Tanase, Solid State Ionics 98 (1997) 229–236.
[5] K. Nomura, T. Takeuchi, S. Tanase, H. Kageyama, K. Tanimoto, Y. Miyazaki, Solid State Ionics 154–155 (2002) 647–652.
[6] S. Li, B. Bergman, J. Eur. Ceram. Soc. 29 (2009) 1139–1146.

[7] K. Kakinuma, H. Yamamura, H. Haneda, T. Atake, Solid State Ionics 140 (2001) 301–306.
[8] Y. Yamamura, S. Kawasaki, H. Sakai, Solid State Ionics 126 (1999) 181–189.
[9] A. Tarancón, A. Morata, F. Peiró, G. Dezanneau, Fuel Cells 11 (2011) 26–37.
[10] D.-S. Byeon, S.-M. Jeong, K.-J. Hwang, M.-Y. Yoon, H.-J. Hwang, S. Kim, H.-L. Lee, J. Power Source 222 (2013) 282–287.
[11] Y. Yamamura, C. Ihara, S. Kawasaki, H. Sakai, K. Suzuki, S. Takami, M. Kubo, A. Miyamoto, Solid State Ionics 160 (2003) 93–101.
[12] Y. Tamai, Y. Kawamoto, Chem. Phys. Lett. 302 (1999) 15–19.
[13] S. Plimpton, J. Comp. Phys. 117 (1995) 1–19.
[14] http://lammps.sandia.gov.
[15] C.A.J. Fisher, M. Yoshiya, Y. Iwamoto, J. Ishii, M. Asanuma, K. Yabuta, Solid State Ionics 177 (2007) 3425–3431.
[16] T.P. Perumal, V. Sridhar, K.P.N. Murthy, K.S. Easwarakumar, S. Ramasamy, Comput. Mater. Sci. 38 (2007) 865–872.
[17] H.-L. Kim, K.-H. Lee, S. Kim, H.-L. Lee, Jpn. J. Appl. Phys. 45 (2006) 872–874.
[18] B. Rambabu, S. Ghosh, W. Zhao, H. Jena, J. Power Source 159 (2006) 21–28.
[19] S.G. Cho, P.F. Johnson, R.A. Condrate, J. Mater. Sci. 25 (1990) 4738–4744.
[20] E.R. Leite, C.M.G. Sousa, E. Longo, J.A. Varela, Ceram. Int 21 (1995) 143–152.
[21] B.I. Lee, R.K. Gupta, C.M. Whang, Mater. Res. Bull. 43 (2008) 207–221.
[22] C.W. Huang, W.C.J. Wei, C.S. Chen, J.C. Chen, J. Eur. Ceram. Soc. 31 (2011) 3159–3169.
[23] M. Burbano, S.T. Norberg, S. Hull, S.G. Eriksson, D. Marrocchelli, P.A. Madden, G.W. Watson, Chem. Mater. 24 (2012) 222–229.